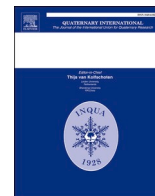




Contents lists available at ScienceDirect

# Quaternary International

journal homepage: [www.elsevier.com/locate/quaint](http://www.elsevier.com/locate/quaint)

## Age, palaeoenvironment, and preservation of prehistoric petroglyphs on a boulder in the oasis of Salut (northern Sultanate of Oman)

Andrea Zerboni<sup>a,\*</sup>, Michele Degli Esposti<sup>b</sup>, Ying-Li Wu<sup>a</sup>, Filippo Brandolini<sup>a</sup>,  
Guido S. Mariani<sup>a</sup>, Federica Villa<sup>c</sup>, Paolo Lotti<sup>a</sup>, Francesca Cappitelli<sup>c</sup>, Marzia Sasso<sup>d</sup>,  
Agostino Rizzi<sup>e</sup>, G. Diego Gatta<sup>a</sup>, Mauro Cremaschi<sup>a</sup>

<sup>a</sup> Dipartimento di Scienze della Terra "A. Desio", Università degli Studi di Milano, Via L. Mangiagalli 34, I-20133, Milano, Italy

<sup>b</sup> UMR 6566, CReAAH, Centre de Recherche en Archeologie, Archeosciences, Histoire, France

<sup>c</sup> Department of Food, Environmental and Nutrition Sciences, Università degli Studi di Milano, Milan, Italy

<sup>d</sup> Italian Mission to Oman (IMTO), University of Pisa, Italy

<sup>e</sup> C.N.R.-I.D.P.A., Via L. Mangiagalli 34, I-20133, Milano, Italy

### ARTICLE INFO

#### Keywords:

Rock art  
Rock weathering  
Microscopy  
Climate change  
Radiocarbon  
Sultanate of Oman

### ABSTRACT

The preservation of rock art in open-air contexts is a global issue controlled by several environmental processes, which are less investigated than the cultural significance of engravings and paintings. For that reason, we discuss the age, preservation, and palaeoenvironmental context of petroglyphs discovered on the flat, almost vertical face of a large boulder fallen along the western slope of Jabal Hammah, a rocky hill that borders the oasis of Salut (northern Sultanate of Oman). Geoarchaeological investigation highlighted that, in the region, the preservation of petroglyphs is due to the interplay of two contrasting weathering processes. On one hand, karst dissolution – even if it is a very slow process in arid and semi-arid lands – gradually levels the surface of boulders. On the other hand, a biomineralized Mn- and Fe-rich rock varnish has developed inside the grooves of the engravings, thus sheltering them from extreme dissolution and promoting the preservation of the pristine shape of the representations. Moreover, organics trapped within the rock varnish have been radiocarbon dated to  $2600 \pm 60$  uncal. years BP. This result allows establishing a limit *ante quem* for the production of these specific engravings and to root it to the Bronze or Iron Age exploitation of the area. This result is of particular relevance in a region where well-dated rock art is virtually absent. Today, the biogeochemical processes leading to the formation of the protective crust are almost inactive, and not consistent with the present dry environmental settings. Their occurrence is in accordance with other local palaeoclimatic record, and suggests Bronze and Iron Age climatic conditions wetter than today. A broader implication of our work is that it shows how a multidisciplinary approach to the study of rock art provides the opportunity of understanding the age of rock art and its paleoenvironmental significance. We demonstrate that physical, chemical, and biological weathering processes are in charge of the preservation and/or destruction of rock art; such processes have to be seriously taken into account in projects of rock art field assessment.

### 1. Introduction

The preservation of rock art in open-air contexts – as much as other cultural heritages (Howard, 2013) – is tricky, especially in locations where extant climatic and environmental settings are different respect to those present at the time of the production of rock art galleries (Darvill and Batarda Fernandes, 2014; Giesen et al., 2014; Groom, 2017). This is especially true in arid and semi-arid regions, where Holocene climatic

changes have deeply and repeatedly reshaped the environment. In such contexts, open-air rock art galleries are, at the same time, a record for past climates as much as a feature threatened by new environmental conditions (Cremaschi et al., 2008; Zerboni, 2012). As a consequence, rock art (paintings and engravings) may suffer strong weathering and taphonomic processes – including physical, chemical, and biological weathering – and in some cases can be completely erased. For these reasons, the understanding of the processes leading to rock art

\* Corresponding author.

E-mail address: [andrea.zerboni@unimi.it](mailto:andrea.zerboni@unimi.it) (A. Zerboni).

<https://doi.org/10.1016/j.quaint.2019.06.040>

Received 27 March 2019; Received in revised form 28 June 2019; Accepted 30 June 2019

Available online 2 July 2019

1040-6182/© 2019 Elsevier Ltd and INQUA. All rights reserved.

preservation and/or destruction and its paleoenvironmental context are as important as its cultural, archaeological, and artistic implications (Whitley, 2005; Dorn, 2006; Dorn et al., 2008; Allen et al., 2011; Bednarik, 2012; Giesen et al., 2014).

Studies promoting the understanding of preservation of rock art preservation and its environmental context remained scanty for a long time. Recently, however, an increased awareness that the understanding of rock art and its decay requires multidisciplinary approaches promoted the development of some projects focused on the assessment of rock art preservation and the study of the interface between rocks and pigments. Some studies considered the many processes affecting rock art and their rock supports (Cerveny, 2005; Hall et al., 2007, 2009; Mol and Preston, 2010; Groom, 2016, 2017; Gallinaro et al., 2018), and applied indices describing the stability of rock art (Dorn et al., 2008; Allen and Lukinbeal, 2011; Groom and Thompson, 2011; Allen and Groom, 2013). In other cases, studies are dedicated to understanding the age and paleoenvironmental significance of rock art (Cremaschi, 1996; Dorn, 2006; Zerboni, 2008, 2012; Bednarik, 2012; Macholdt et al., in press). For that reason, in this paper we examine some engravings recently discovered in the northern part of the Sultanate of Oman (oasis of Salut), with the main aim to decipher their age and significance in relation to the local and regional archaeological background, and to reconstruct the main environmental processes leading to the decay or preservation of petroglyphs.

Several petroglyphs' panels were discovered in the region and the

most of them show the same slightly varnished, usually dotted pecking technique, and the same iconographic repertoire commonly witnessed in other parts of the Arabian Peninsula (e.g., Jung, 1994; de Ceuninck, 1998; Ziolkowski, 1998, 2007; Bednarik and Khan, 2002; Khan, 2007, 2013; Bednarik, 2005, 2017; Fossati, 2017). However, the finding discussed here represents a so far unique discovery within the regional archaeological context and deserves a specific geoarchaeological investigation. In fact, this rock art panel comprises a series of engravings that differs in pecking technique from the most widespread ones, and notably from the large majority of the rock art present in the same oasis. Although being generally strongly abraded by environmental processes, where they are sheltered by a dark, biomineralized rock crust, they are better preserved. The same rock crust allowed dating engravings and elucidating their palaeoenvironmental history.

## 2. The study area

### 2.1. Geographic, climatic and geologic background

The rock art panel here investigated consists of engravings on a limestone boulder outcropping on the southern slope of a hill belonging to Jabal Hammah, in the vicinity of the archaeological site of Salut (Fig. 1) in the northern Sultanate of Oman (Degli Esposti et al., 2018b). The Geologic Map of Oman, 1:250,000, sheet NF4007 – NIZWA, reports the toponym Jabal Hammah, although locals currently refer to the same

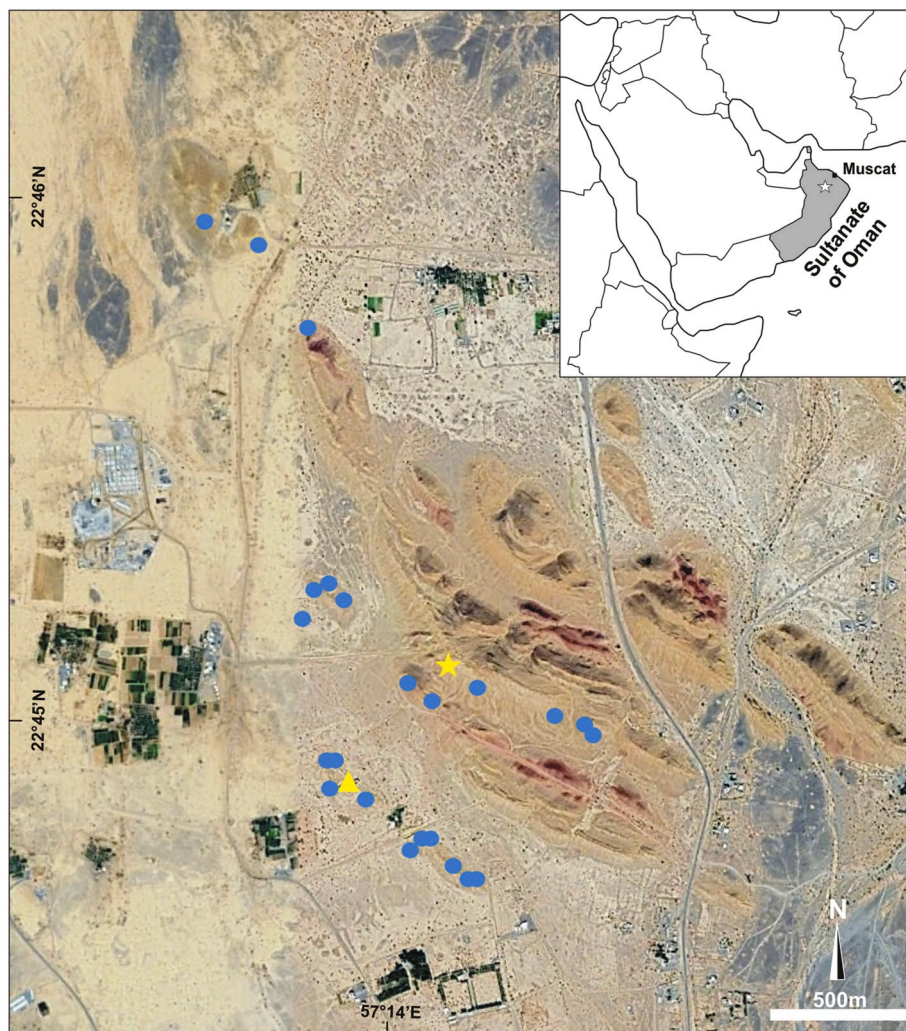


**Fig. 1.** The study area on GoogleEarth™ satellite imagery; the star is the position of the boulder, dots are other rock art stations, the triangle is the position of the citadel of Salut. Note the monocline pattern of the Jabal Hammah. The inset indicates the position of the area in the Sultanate of Oman.

hill as Jabal Salut, which is the toponym used in most of the archaeological literature cited here. The area is located between the modern villages of Bisya (2 km to the South) and Bahla (20 km to the North), and stands at the margin of the palaeo-oasis of Salut, which developed in the Early and Middle Holocene along Wadi Sayfam (Cremaschi et al., 2018a). A variety of sedimentary, metamorphic, and igneous rocks outcrop in this region (Geologic Map of Oman, 1:250,000, sheet NF4007 – NIZWA); the area is delimited to the North by the massif being part of the Mid-Late Cretaceous Samail Ophiolite, and to the West and to the South by Permian to Cretaceous sedimentary formations (limestone and radiolarite). The bedrock of the hill hosting the engraved boulder consists of the Late Jurassic to Cretaceous Wahrah Formation (Glennie et al., 1974), which includes lithoclastic, oolitic, marly limestone, chert, and silicified limestone (Béchenec, 1986). Pleistocene and Holocene deposits cover part of the region, including large alluvial fans and fine sediments covering most of the bottom of the alluvial plain along the main wadis (see details in Cremaschi et al., 2018a).

The present climate of Northern Oman is arid to semi-arid and controlled by the seasonal development of the monsoon winds. Rainfall originates from Mediterranean frontal systems in winter and spring (Weyhenmeyer et al., 2000, 2002), and varies between 150 and 250 mm/yr (Alsharhan et al., 2001; Fleitmann et al., 2007). On the contrary, palaeoclimate studies based on speleothems from the Hoti Cave (at ca. 45 km from the study site; Neff et al., 2001; Fleitmann et al., 2007) suggest that in the early Holocene (between ca. 10.5 and 9.5 ka BP) precipitations increased, triggered by the northward shift of the mean latitudinal position of the summer ITCZ and the associated Indian Summer Monsoon (ISM) rainfall belt. After ~7.8 ka BP to present, the mean summer ITCZ continuously migrated southward triggering the gradual decrease in intensity and duration of the ISM season. Other records from southern Oman and Socotra suggest a marked decrease in precipitation at ca. 2 ka BP, thus confirming a general decrease in intensity of the Indian Ocean monsoon in the late Holocene (Fleitmann et al., 2007). Cremaschi et al., 2015

## 2.2. Archaeological background

The archaeological record of the region of the Sultanate of Oman roughly comprised between the cities of Nizwa and Bahla was initially surveyed in the 1970ies (Hastings et al., 1975; De Cardi et al., 1976), but systematic archaeological investigation started later (e.g. Orchard and Orchard, 2002). A project of extensive archaeological research which entailed the excavation of the major archaeological sites in the oasis (Husn Salut; Salut-ST1; Jabal Salut necropolis; Qaryat Salut) was established in 2004, when the work of the Italian Mission to Oman started tracing the outlines of the regional evolution of human occupation (Phillips et al., 2015; Degli Esposti, 2015a; Avanzini and Degli Esposti, 2018; Tagliamonte and Avanzini, 2018). Extensive stratigraphic excavations were combined with a programme of surveys conducted over the plain surrounding the sites, as well as the surrounding hillocks (e.g. Phillips et al., 2012; Condoluci et al., 2014), which led to the identification of several open-air sites, including some rock art panels and isolated representations (Fig. 1).

Locally, the earliest human traces in the area can be dated back to the Palaeolithic, whereas scatters of lithics suggest the Neolithic exploitation of the region (Fig. 2). However, the most evident and systematic occupation of the area and exploitation of natural resources corresponds to the Early Bronze Age (second half of the 3rd millennium BCE). At that time, three monumental stone tower sites were erected along the eastern side of Wadi Sayfam, being an expression of a specific culture that displays homogeneous characters throughout the Oman peninsula, from Musandam in the north to the Masirah Island in the south (Orchard and Stanger, 1994; Degli Esposti, 2016). A demographic decrease apparently marked the first half of the 2nd millennium BCE, while a reverse trend started around the end of the 15th century BCE, as indicated by the establishment of a dense network of Iron Age sites, clustering around the

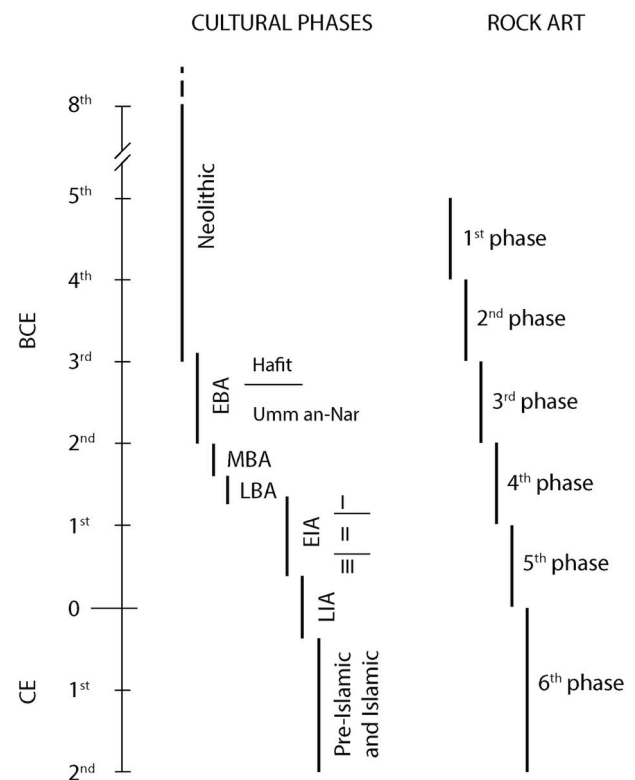


Fig. 2. Regional cultural periods on the basis of the current archaeological literature, compared with the periodization of rock art in Oman (Jabal Akhdar) as suggested by Fossati (2017).

citadel of Salut (Avanzini and Phillips, 2010; Phillips et al., 2010; Condoluci et al., 2014). Archaeological excavation suggests that this settlement, somehow precocious compared to other areas of southeast Arabia, lasted beyond the end of the Early Iron Age period, that is, beyond c. 300 BCE and likely until the 1st century CE (Degli Esposti et al., 2018a, 2019). During this long phase, the palaeo-oasis of Salut reached its greatest spatial extent and apogee of agricultural land use. Around the end of the 1st century CE, the palaeo-oasis of Salut was abandoned for several centuries. After that, the citadel of Salut witnessed three distinct periods of Islamic occupation: (i) Early Islamic (ca. 9th/10th century CE); (ii) Middle Islamic (ca. 12th/13th century CE); and (iii) Late Islamic (after the 16th century CE) (Whitcomb, 1975; Avanzini et al., 2005; Avanzini and Degli Esposti, 2018). Geo-archaeological evidence indicates that the major phases of expansion of settlements in the area were related to the establishment of efficient systems for water management sustaining intensive cultivation (Cremaschi et al., 2018a).

## 3. Materials and methods

### 3.1. Description of the rock art panel

The petroglyphs discussed in this paper were engraved on the vertical flank of a large boulder on the southwestern slope of Jabal Hammah (Figs. 3 and 4), northeast of Husn Salut. The Jabal Hammah is a rocky monocline relief dotted by several prehistoric tombs (Condoluci and Degli Esposti, 2015; Degli Esposti et al., in press). On the southwestern slope of the hill, several blocks and boulders belonging to the Wahrah Formation are present, corresponding to the remains of an ancient rockfall triggered by undersapping processes that eroded the underlying marls. In the central part of the rockfall, the engraved boulder stands up. Several smaller blocks stand at its foot, possibly adjusted to increase its stability or to allow carving the engravings (Fig. 4). Other large boulders

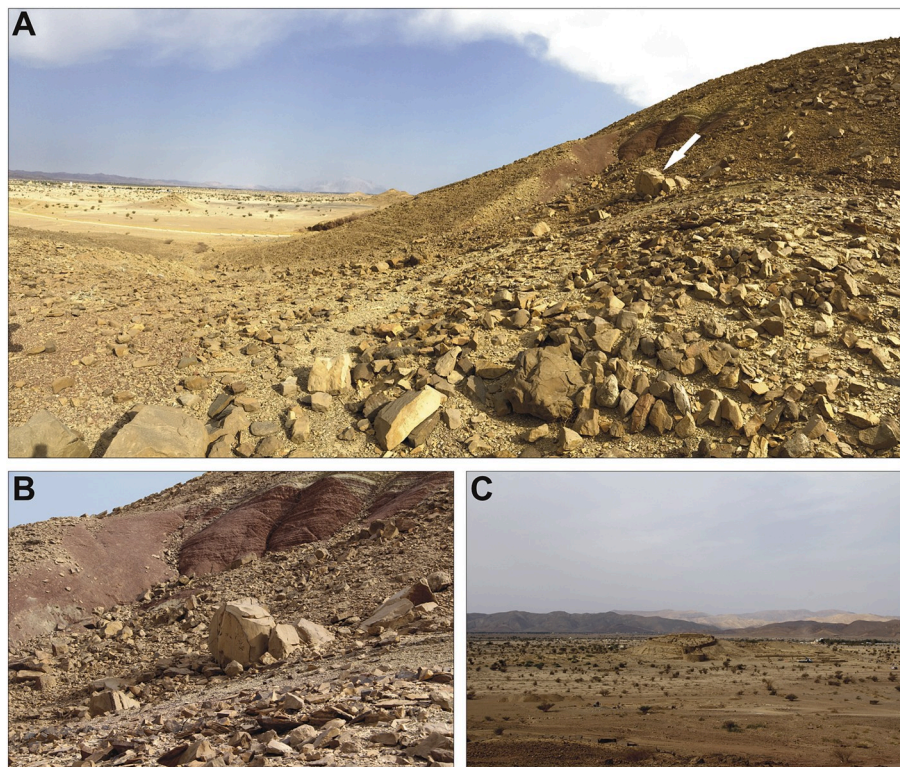


**Fig. 3.** (A) General view of the western slope of the Jabal Hammah (the arrow indicates the position of the boulder). (B) A detail of the slope with the engraved boulder in its present-day landscape. (C) A view of the citadel of Salut from the Jabal Hammah.

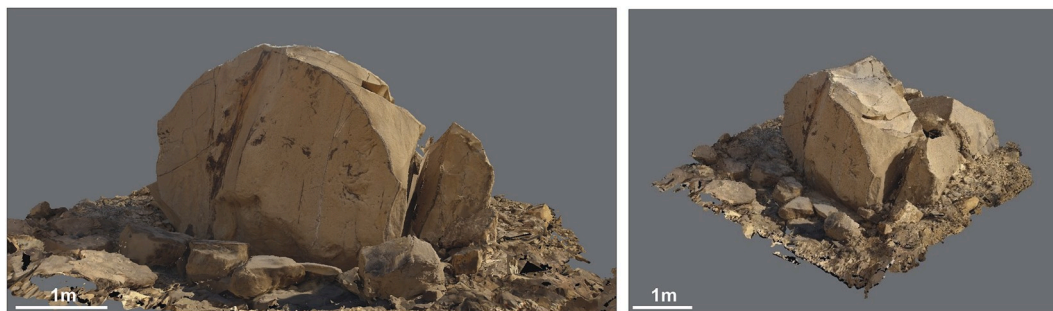


**Fig. 4.** Different views of the engraved boulder after 3D reconstruction (see the text for details).

found along the slope of the hill were artificially stabilised, but they do not display engravings. On the contrary, in the same area several small, isolated engraved blocks were found. The large boulders and the small ones possibly correspond to a sort of landmark and are part of the same archaeological landscape.

We distinguished three engraved figures carved on the boulder surface (Fig. 5). Despite two of them being remarkably less well preserved, all can be recognised as representing the same motif: a standing man holding in his right hand a long shaft ending in a hemi-circular item, possibly the representation of a halberd (henceforth we refer to this item as halberd). The three figures are sketchily made with simple traits (“stick men”), with outstretched arms and open legs. On the best-preserved figure, the uppermost, a faintly visible vertical stroke may indicate the penis, which is also vaguely visible in the central figure. The engravings were made with a continuous pecking, lowering the engravings’ grooves of a few millimetres under the original surface.

Other petroglyphs are scattered in the surroundings of Jabal Hammah and they include horse riders, various animals, and several signs. The most of the latter are common in the region, as suggested by several

comparisons (e.g., Jung, 1994; de Ceuninck, 1998; Haerinck, 1998; Ziolkowski, 1998, 2007; Khan, 2007, 2013; Fossati, 2017). Although other examples of complete motifs of the standing man with halberd have not been found so far in the area of Salut, we spotted a few representations of the single halberd (Fig. 6). Interestingly, these engravings were made using the continuous pecking technique instead of the dotted technique that distinguishes the great majority of the rock art in the area; this is a further similarity to our case study. Three isolated halberds are on the southern face of a boulder employed in the building of one of the structures that is part of an Early Bronze Age tower (T2) standing some 600 m north of the Iron Age complex of Salut (Degli Esposti, 2015b). The engraving was manufactured after the block was inserted in the masonry structure; however, it is hard to define the real chronological correlation between the engravings and the age of the tower T2. A few stone seals found during archaeological excavations provide additional, indeed scarce, parallels. A cylinder seal found at the Bronze Age tower ST1 in the area of Salut, dated to the Iron Age re-occupation of the site, bears a representation closely resembling the halberds shown on the discussed boulder (Degli Esposti, 2012, 2015b).

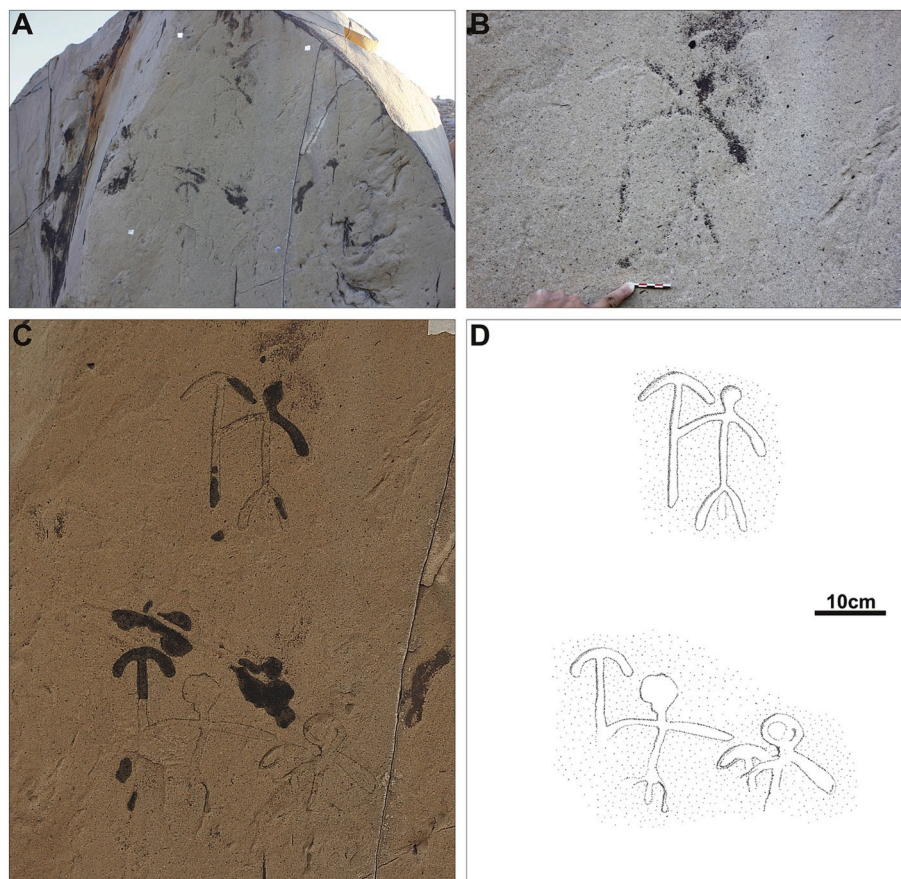


Fig. 5. (A) Pictures of the main panel of engravings representing men with halberd, and (B) a detail of the best preserved figure. (C, D) Interpretative drawing of the panel of men with halberd.

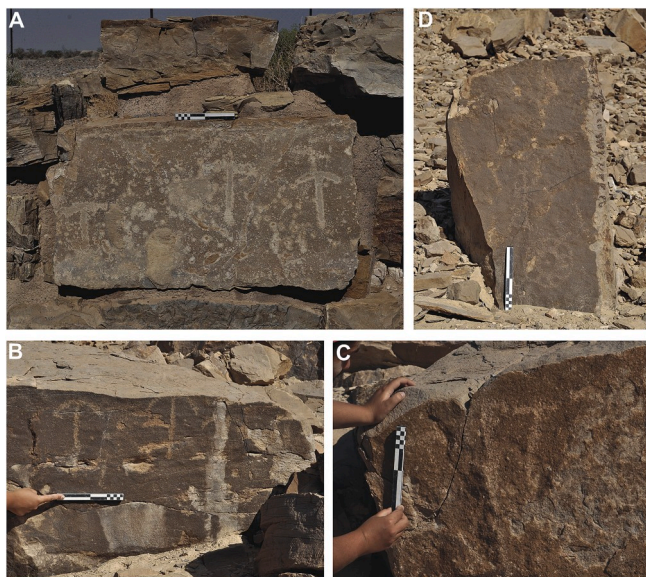


Fig. 6. (A–C) Local comparisons for the representation of men with halberd; (A) represents the engravings found on the masonry of the Bronze Age tower T2. (D) An example of a different iconography in the local rock art.

Moreover, another cylinder seal from Ra'a al Jinz RJ-2, dated by its excavators between 2500 and 2250, is carved with an identical figure (Cleuziou and Tosi, 2000).

### 3.2. Field survey, photographic recording, and analyses

The engraved boulder discussed here was located by one of the authors (MC) during a survey of the rock art panels over the hills surrounding the citadel of Salut. The boulder and the surrounding area were carefully inspected and engravings digitally recorded and drawn. Moreover, a 3D model of the boulder was elaborated with Structure-from-Motion (SfM) photogrammetry. This technique uses an automated process to obtain point clouds, triangular meshes and full 3D textured models from images (Peña-Villasenín et al., in press) and has been applied with relevant results in field archaeology (De Reu et al., 2013; Galeazzi, 2016; Waagen, 2019) as well as in rock art studies (Sanz et al., 2010; Plisson and Zotkina, 2015; Robert et al., 2016; Bea and Angás, 2017), being the most appropriate solution for macroscopic 3D recording in the field in terms of time and cost of execution. Moreover, for the majority of rock art sites, SfM 3D-modelling has proved to be a valuable, cost-effective alternative to Terrestrial Laser Scanner (TLS) (Johnson and Solis, 2016; Jalandoni et al., 2018). In this paper, we applied a low-cost and high flexible SfM approach (Jalandoni et al., 2018) to elaborate a 3D model for metric analysis and digital tracing of rock art motifs (Supplementary Material). In our case study, we took 156 pictures with a Canon EOS 100D from different perspectives and elevations with at least 60% overlap and markers with a known distance were placed near the boulder; Table 1 presents camera location parameters used in the elaboration of the 3D model. The 3D model was generated and scaled using Agisoft Metashape photogrammetric software (Agisoft, 2018).

As described in the following parts (sections 4.1 and 4.2), the best-preserved part of the rock art panel is covered by a dark, hard mineral coating. The same coating covers or fills small natural depressions along

**Table 1**

Camera location parameters used to generate the 3D model of the boulder with rock art.

Number of pictures	156	Camera stations	156
Altitude	2.67 m	Tie points	128,354
Ground resolution	0.647 mm/pix	Projections	400,483
Coverage area	13 m <sup>2</sup>	Reprojection error	1.48 pix

the boulder and along vertical discontinuities (fractures). To establish the nature and age of the weathering crust, we collected it in correspondence of several linear fractures on the sides of the boulder not related to engravings. Several small crust and bedrock samples were removed with a small chisel.

Rock samples were cut perpendicular to the crust surface, polished, and thin section prepared according to the procedure described in Murphy (1986). Micromorphological observation under plane-polarized light (PPL) and cross-polarized light (XPL) of thin sections were conducted with an optical petrographic microscope Olympus BX41 equipped with a digital camera (Olympus E420); during interpretation, we followed the concepts discussed in Cremaschi et al. (2018b). Micromorphological studies of thin sections also employed a Cambridge 360 scanning electron microscope (SEM) imaging both secondary and back-scattered electrons. Energy dispersive X-ray analysis (EDS Link Isis 300) required to carbon coat the thin sections. Energy dispersive X-ray spectroscopy worked with an accelerating voltage of 20 kV, filament intensity 1.70 A, and probe intensity of 280 pA. Every analysed element was previously standardised by using several single element standards (Micro-Analysis Consultants Ltd); elemental concentrations measured by EDS are reported as oxide weights normalized to 100%.

Several fragments of the crust were collected and glued on glass fibers mounted on a goniometer head. An Oxford Diffraction Xcalibur 4-circle diffractometer, equipped with a Mo-K $\alpha$  X-ray tube ( $\lambda = 0.7107 \text{ \AA}$ ) and a CCD area detector, operating at 50 kV and 30 mA, was used for X-ray diffraction investigations. The diffraction patterns were collected by exposing each sample for 45 or 120 s during a full rotation of the goniometer head around the vertical axis. The collected images were integrated into a 2 $\theta$ -Intensity diffraction pattern adopting the routines implemented in the software CrysAlis (Rigaku Oxford Diffraction, 2018). The phase assignment was done based on the collected powder diffraction patterns, using the 'Xpert HighScore suite (Degen et al., 2014).

Several samples of rock crust were observed with a Confocal Laser Scanning Microscope (CLSM) after fluorescent staining. Confocal images were collected using a Nikon A1 laser scanning confocal microscope and a 20x/0.75NA (WD 1 mm) Plan Apo  $\lambda$  objective. Fluorescence was excited and collected using different combinations of the following laser lines and emission parameters: (i) autofluorescence from photosynthetic pigments was viewed in the red channel using the 633 nm line of an Ar/HeNe laser in the emission range of 650–750 nm; (ii) The total biofilm biomass was visualized by DAPI (4',6-diamidino-2-phenylindole, Invitrogen) staining according to manufacturer instructions. This dye was excited with a 405 nm laser with emission collected in the range of 430–480; (iii) metabolically active cells of the biofilms were viewed in the green channel by staining the samples with Calcein AM (Film-Tracer™ calcein green biofilm stain, Invitrogen) according to manufacturer instructions. This dye was excited with a 488 nm laser with emission collected in the range of 500–550 nm; (iv) extracellular polysaccharides were detected by Con A staining (Concanavalin A, Alexa Fluor 488 conjugate, Invitrogen) according to manufacturer instructions. This dye was excited with a 488 nm laser with emission collected in the range of 500–550 nm; (v) extracellular proteins were detected by Bodipy staining (BODIPY® 630/650-X, Invitrogen) according to manufacturer instructions. This dye was excited with a 633 nm laser with emission collected in the range of 650–700 nm. CLSM was used in reflectance mode with the 488 nm argon line for relief

imaging of specimens. Captured images were analysed with the software NIS-Elements (Nikon) for 3D reconstructions of biofilms.

Based on both SEM and optical microscopes observations, one sample of weathering surface not experiencing mechanical or biogeochemical weathering (Sowers, 2000) was selected for accelerator mass spectrometry radiocarbon dating (AMS-<sup>14</sup>C), as organic carbon generally occurs trapped under the Mn-rich rock varnish at the rock interface (Dorn et al., 1989). The sample for dating was prepared according to the protocol described in Zerboni (2008). A portion of the same sample was analysed for total organic carbon (TOC) by titration using chromic acid to measure the oxidizable organic carbon (Walkley and Black, 1934). The sample was dated at the facility of the University of Georgia (USA). AMS-<sup>14</sup>C age result was calibrated using the INTCAL13 calibration curve (Reimer et al., 2013) and results reported with 95.4% and 68.2% accuracy (Table 2).

## 4. Results

### 4.1. Description of the rock surface of the boulder

The surface of the boulder, as much as many other rock surfaces in the area, displays evidence of weathering processes. Physical and chemical deterioration are the most evident effects of weathering. In the area, blocks are often disaggregated by thermal stress, and the surface of limestone rocks dotted by small-scale solution pits, karren, and microkarren (*sensu* Ginés et al., 2009) (Fig. 7). One further karst-related feature is evident at the micro-scale (Fig. 8); under the microscope, boulders and blocks display dissolved surfaces with etch pits (Fiol et al., 1992). In this case, where the dominant lithotype is a siliceous limestone, the formation of alveolar micro-depressions at the rock surface is controlled by the dissolution and removal of micritic mud among silicified grains (Fig. 8). Moreover, on the considered boulder evidence of calcium carbonate-bearing case hardening (Smith, 1988; Dorn, 1998) is present. In fact, along the margins of the boulder, we occasionally observe the occurrence of a few mm thick coating of sparitic calcite combined with iron oxides and occasionally clay minerals (Fig. 8).

As a consequence of the abovementioned processes, the surface of the boulder is rough and limestone dissolution levelled the micro-relief of engravings, leading to their removal. The groves of the engravings are best preserved in few places, where dark, few mm-thick crusts are present (Fig. 9). The same crust is evident also in correspondence of natural depressions, cracks, and fractures along the same boulder, and on many other rocks outcropping along Jabal Hammah (Fig. 9). At the macro-scale, the crust is metallic, smooth, massive, and hard; its Munsell® (1994) color varies between 10R 2.5/1 and 10 YR 2/2 (reddish black–very dark brown). Moreover, a very thin layer of a darkish coating covers the whole rock surfaces of subaerially exposed rocks (Fig. 7). Generally, the color of this coating is 10 YR 4/1 (dark gray) and contrast with the yellowish color of the fresh Wahrah Formation limestone (10 YR 7/6, yellow). The thin rock coating is widespread in the area, but at some places dismantled by recent wind erosion.

Under the petrographic microscope, the dark crust consists of a continuous layer draping the discontinuities between the residual siliceous grains and filling the alveolar depressions at the rock surface (Fig. 10). This results in an irregular thickness of the crust along the rock surface, higher in correspondence of alveolar voids and thinner on grains. At PPL and XPL, the dark coating is massive and opaque, with a few reddish reflections along some silicified ooids; reddish parts of the coating show a moderate birefringence under XPL. Conversely, the thin rock coating widespread on all exposed rock surfaces displays almost the same thickness of a few tens of microns (rarely thicker) and a dark brownish color under PPL to a light to dark brown color and very weak birefringence under XPL (Fig. 8). This coating covers also the dark crust and has analogies with dust films (Rivard et al., 1992; Dorn, 1998) enriched with local constituents and others originating from the aerosol.

The higher magnification of the SEM better illustrates the occurrence

**Table 2**  
AMS-<sup>14</sup>C dating results on rock crust; calibration according to Reimer et al. (2013).

Sample	Latitude	Longitude	TOC (g/ Kg)	Laboratory code	$\delta^{13}\text{C}$	pMC	AMS <sup>14</sup> C age years uncal BP	AMS <sup>14</sup> C age cal. 95.4%		AMS <sup>14</sup> C age cal. 68.2%	
								years cal BC	years cal BP	years cal BC	years cal BP
Salut 1	N25°54'38.8"	E 12°14'48.9"	1.45–1.5	UGAMS 32708	–25.34	72.39 ± 0.52	2600 ± 60	901–541	2850–2490	836–590	2785–2539



**Fig. 7.** Some examples of limestone surfaces displaying evidence of karst dissolution. Arrows in A and B indicate the deepest micro-karren (linear features); arrows in B and C indicate dissolution surfaces marked by small and irregular depressions C.

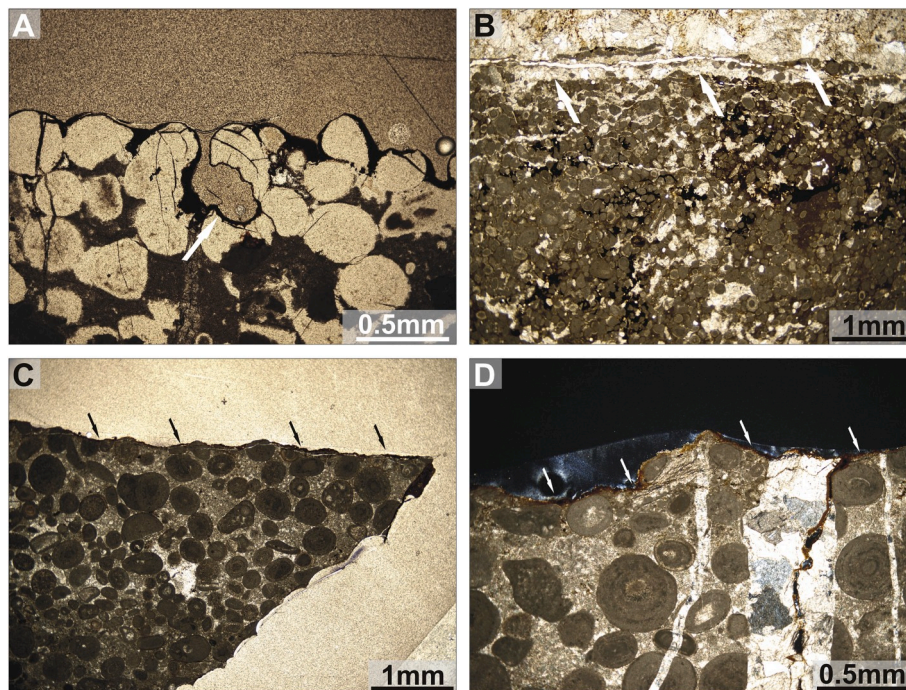


**Fig. 8.** Optical images of a cross section of samples from the engraved boulder: (A) Alveolar micro-depressions at the rock surface, note the dissolution of micritic mud (PPL). (B) Sparitic calcite of the case hardening (XPL). (C) Cross section of a limestone surface covered by the thin dust film (PPL) and (D) a detail of the dust film (XPL).

of alveolar voids due to dissolution on top of rock surfaces (Fig. 11), the continuity of the thin dust film (Fig. 11), and the occurrence of coating infilling and draping discontinuities (Fig. 12). The thickness of the dust film never exceeds 100  $\mu\text{m}$  and is dark brown under the SEM; the EDS analysis suggests a composition dominated by Si (~50–60%), Al (~16–20%), Fe (~9%), and Mg (~8–11%), and enrichments of such alkalis as K (~2.5–5%) and Na (~2–2.5%). This layer adheres to the rock surface, but it did not tightly grow on it (Fig. 11); chemical data suggest that this layer consists mostly of clay minerals, possibly Fe-oxides stained, and enriched in alkalis from the aerosol (Zerboni, 2008), thus confirming the attribution to dust film. The thickness of the dark crust found in the engravings' furrows and sampled along discontinuities of the block varies from a few up to 500  $\mu\text{m}$ . SEM images in Fig. 12

illustrate the different properties of the samples and help in discriminating between the micritic matrix, siliceous ooids, and many components of the crust. The outer part of the crust consists of a convolute to botryoidal mixture of crystals; EDS analysis detected major concentrations of the following elements: Si (~36–44%), Al (~17–20%), Fe (~10–13%), Mg (~6.5–10%), K (~3%), Na (~2.5%), and Ca (~2.5–1.5%). This layer is up to 100  $\mu\text{m}$  thick and dotted by whitish features enriched in Mn (~7–16%); it can be interpreted as a layer of clay minerals enriched in Mn and Fe oxides – a rock varnish (Dorn, 1998, 2007). The subsequent part under the SEM appears white and bright; in fact, it is enriched in Fe (~85–90%), with a lower content of Si (~8%), Na (~1.5%), Mg (~1%), and Al (<1%). Towards the bottom of the crust, the Fe content decreases to ~65%, but we noticed an enrichment of Ca

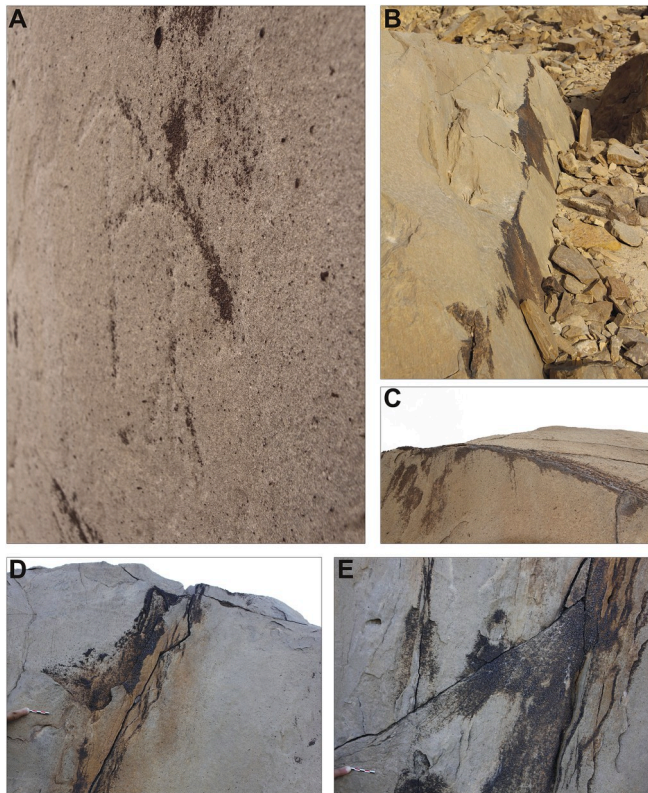


**Fig. 9.** Field pictures of the rock crust developed in the groves of one of the engraved figures (A); note the incoming inversion of the relief due to karst dissolution and the crust sheltering the engraving from complete levelling. (B–E) Examples of the same crust developed elsewhere on the same boulder.

(~7.5%), and P (~5.5%). In rock coatings, concentrations of Ca and P showing parallel trends generally indicate the presence of calcium phosphates minerals, ultimately related to biologic processes (Reneau et al., 1992; Dorn, 1998; Zerboni, 2008).

The analysis of the X-ray powder diffraction patterns reveals a heterogeneous spatial distribution of the mineral phases making up the weathering crust. Overall, in addition to the ubiquitous contribution of quartz, which can be assigned to the underlying siliceous ooids, the observed diffraction peaks from the collected patterns were assigned to birnessite – ideally  $(\text{Na,Ca,K})_{0.5}(\text{Mn}^{4+},\text{Mn}^{3+})\text{O}_4 \cdot 1.5\text{H}_2\text{O}$  – and, locally, hydroxyapatite and halite, whereas two samples clearly show also the occurrence of an amorphous phase. The identification of amorphous phases is compatible with the occurrence of mixtures of Mn and Fe oxides and hydroxides that are common in rock coatings, whereas birnessite is one of the most common crystalline phases in Mn-bearing rock varnish (Potter and Rossman, 1979; Dorn, 1998). The detection of hydroxyapatite is compatible with the occurrence of Ca and P, and has been described in rock varnish (Nriagu, 1984; Dorn, 1998).

**4.2. CLSM observations**

Representative images of the biofilm biomass and the extracellular organic matter (EOM) retrieved on the rock surfaces are presented in Fig. 13a and Fig. 13b respectively. The images correspond to the Maximum Intensity Projection (MIP) 3D reconstructions obtained from confocal images series with the dedicated NIS-Elements software.

The fluorescent signals in Fig. 13a visualise cells in the biofilms. It is possible to observe a patchy distribution of small cell aggregates following the topography of the rock surfaces. Phototrophs (red signal) appear as few isolated coccoid cells on the rock surfaces, while chemotrophs (green + blue signals) dominate the biofilm community. The fraction of metabolically active cells in the biofilms is distinguished by coupling the results from DAPI staining (blue signal) with those obtained from Calcein AM staining (green signal) (Fig. 13a). In fact, while the DNA-binding dye DAPI shows the total biofilm biomass (active and non-active cells), the green fluorescent viability dye Calcein AM can measure intracellular esterase activity, which is an indicator of both cellular metabolic activity and cell membrane integrity. Thus, the green signal in Fig. 13a represents the fraction of active cells in the biofilm, which is about 30% of the total biomass. The fluorescent signals in Fig. 13b indicate the EOM retrieved on the rock surfaces. The green signal, derived from the lectin-binding dye Con A, reveals the presence of

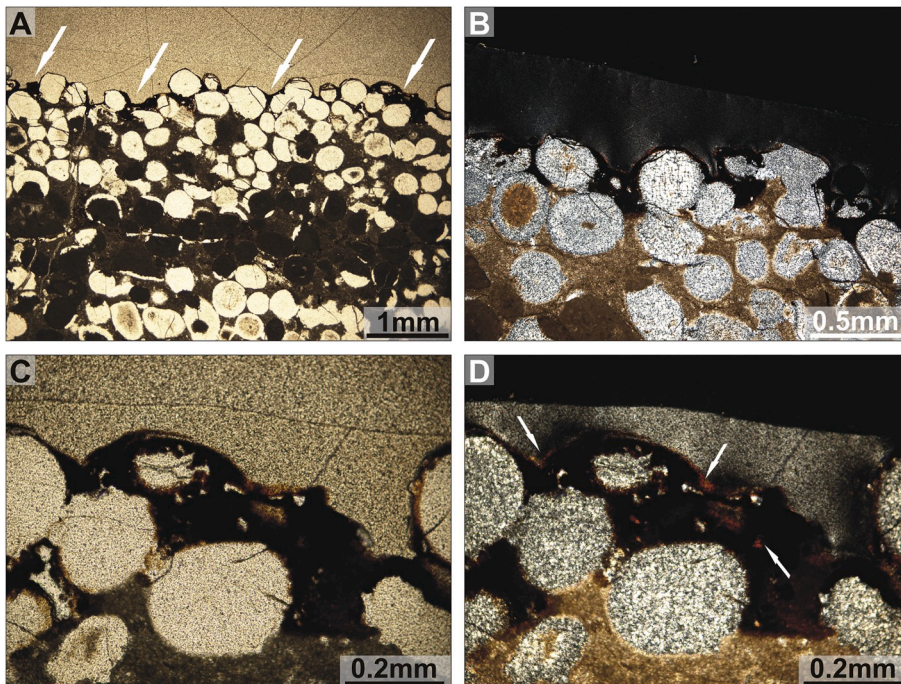


**Fig. 10.** Optical images of a cross section of samples of rock crust. (A) General view illustrating the distribution of the crust draping silicified ooids and infilling voids among them (PPL). (B) A detail of the crust in XPL illustrating its optical properties; note the occurrence of completely and partially silicified ooids and the removal of part of the micritic mud due to dissolution. (C) The crust at high magnification illustrating intergranular spaces filled by varnish material (PPL). (D) The same in XPL, note the presence of reddish and birefringent material (indicated by the arrows).



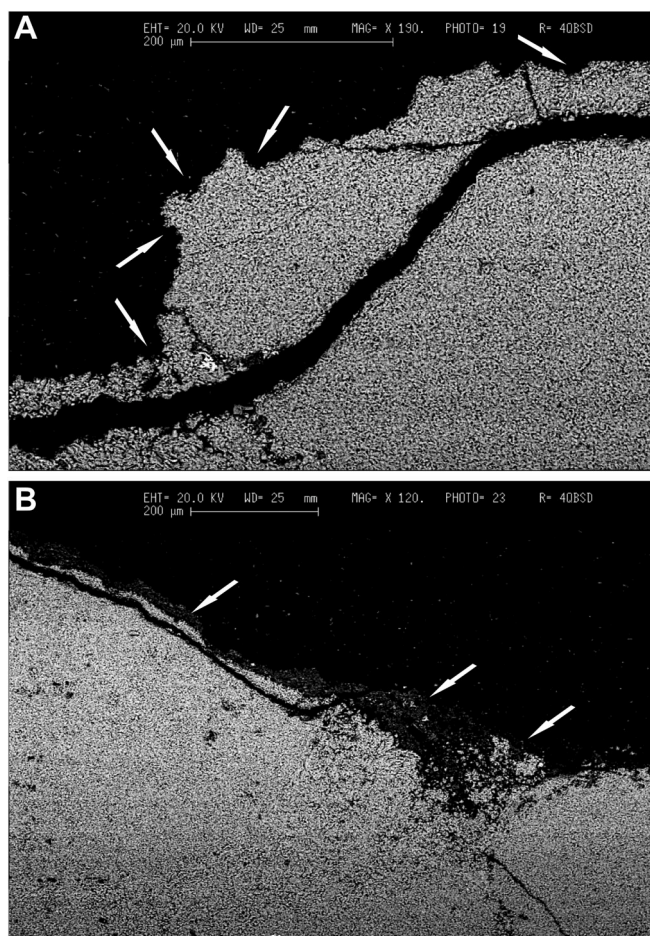


**Fig. 11.** Scanning Electron Microscope images of a cross section of rock surface: (A) alveolar voids due to dissolution (etching pits are indicated by the arrows); (B) thin dust film indicated by the arrows.

extracellular glycoconjugates (i.e. polysaccharides, including those ones covalently linked to proteins and/or lipids) covering the lithic surfaces. BODIPY® 630/650-X is an amine-reactive dye used to label the primary amines of proteins, amine-modified oligonucleotides, and other amine-containing molecules. The resulting red signal shows the presence of extracellular proteinaceous materials accumulating on the rock surfaces and partially overlapping the green signal of glycoconjugates.

Overall, the microbiological investigations reveal that: i) the lithic substrates are colonised by a monolayer of cells growing in small clusters that follow rock fissures and cracks; ii) chemotrophs comprise the largest proportion of the biofilm community in all the specimens analysed, and iii) only a small fraction (about 30%) of the biofilm community is metabolically active; moreover, iv) a thin layer of extracellular organic materials rich in glycoconjugates cover most of the rock surfaces.

#### 4.3. Radiocarbon dating

Rock varnishes and rock crusts can be radiocarbon dated if they are biomineralized and if they still preserve organics trapped within weathering products (Dorn et al., 1989, 1992; Zerboni, 2008). The latter generally act as a sealing, allowing the isolation of the carbon systems from external contaminations. A sample of crust collected on the boulder – although not in correspondence of engravings – displaying a TOC content of ca. 1.5 g/kg was submitted to AMS-<sup>14</sup>C dating. The analyses rendered the age of 2600 ± 60 uncal. years BP (see calibration in Tab. 2). This age refers to the growth of the rock crust; thus it is a limit *ante quem*

for the making of engravings.

## 5. Discussion

### 5.1. Engravings in the regional context

In recent years, a number of studies highlighted the rich rock art record of the Arabian Peninsula (e.g. Anati, 1968-1974; Ash Shari, 1994; Nayeem, 2000; Crassard, 2013; Jennings et al., 2013; Bednarik, 2017; Guagnin et al., 2017), and in particular of the Sultanate of Oman (e.g. Clarke, 1975a, 1975b; Preston, 1976; Jackli, 1980; Insall, 1999; Yule, 2001; Khan, 2007; Al-Jahwari and ElMahi, 2013; Fossati, 2017; Tokunaga et al., 2019). Nevertheless, the engravings of human figures with halberd are almost unique in the region; at least, a few engraved items that can be interpreted as isolate halberds exist. In fact, no fitting comparison is known from South East or South Arabia. One similar engraving was found north of Timna in the Arabah Valley (Negev Desert), among the representations of a densely decorated panel with petroglyphs belonging to different ages (Rothenberg, 2001). At this site, a “stick man” in the same outstretched position as those at Salut and holding a double-pointed-head item is present. This figure has some similarities with the one represented at Salut. However, the head of this item (tool or weapon) is less curved, and the man holds it from one end of the head and not from the shaft. Given the archaeological context of the famous mining area of the Arabah (e.g. Rothenberg, 1972; Rothenberg et al., 1978), this tool could be reasonably interpreted as a pickaxe.

### 5.2. Formation of rock coatings

The microscopic, chemical, and mineralogical investigation on the rock surface of the boulder with engravings and the identification of an equivalent of the rock crust preserving engravings suggests the occurrence, along time, of many and contrasting weathering processes. Different climatic conditions triggered each weathering process and led to the formation of specific weathering products.

The dissolution of the rock surfaces and the formation – at the micro-scale – of alveolar etching pits are related to karst process. This requires moderate water availability, higher than the present day one. In fact, the effects of karst processes along Jabal Hammah seem quite significant and not compatible with the present hydroclimate. In fact, the so-called arid karst is controlled by intense evapotranspiration at the surface, low rate of CO<sub>2</sub> enrichment of solutions, and fast percolation of water, resulting in less intense surface karstification and more intense underground dissolution (Kranjc, 2010). The greyish layer covering all sub-aerially exposed rock surfaces in the area of Jabal Hammah is a dust film (Dorn, 1998), consisting of fine mineral particles originating from the aerosol and the deflation of surrounding soils aggraded on rock by the wind. Its accretion is related to arid environmental conditions and today its formation could be still active.

Finally, the crust grown along the engravings’ furrows can be defined as a complex and multi-layered Fe- and Mn-bearing rock varnish. Its formation required several processes including microorganism-promoted biomineralization. The distribution of this weathering surface is more limited than the dust film, and it seems to be more common on the sheltered portions of siliceous limestone. This is compatible with other data suggesting that rock varnish growth occurs preferentially on silica-bearing rocks (Dorn, 1998, 2007). At Salut, rock varnish consists, like many varnishes developed in warm deserts, of a thick accumulation of poorly layered and oxides-impregnated clay minerals. In our case, a large part of the rock varnish is impregnated by Fe-oxides, which represents the central part of the varnish, whereas its outer part mostly consists of the classical Mn-rich rock varnish. The association of iron films with manganese-rich accretions is common in arid and semiarid regions (e.g., Engel and Sharp, 1958; Hooke et al., 1969; Hein and Koski, 1987; Cremaschi, 1996). Both iron and manganese oxides are likely the result of intense biomineralization occurred in presence of clays under

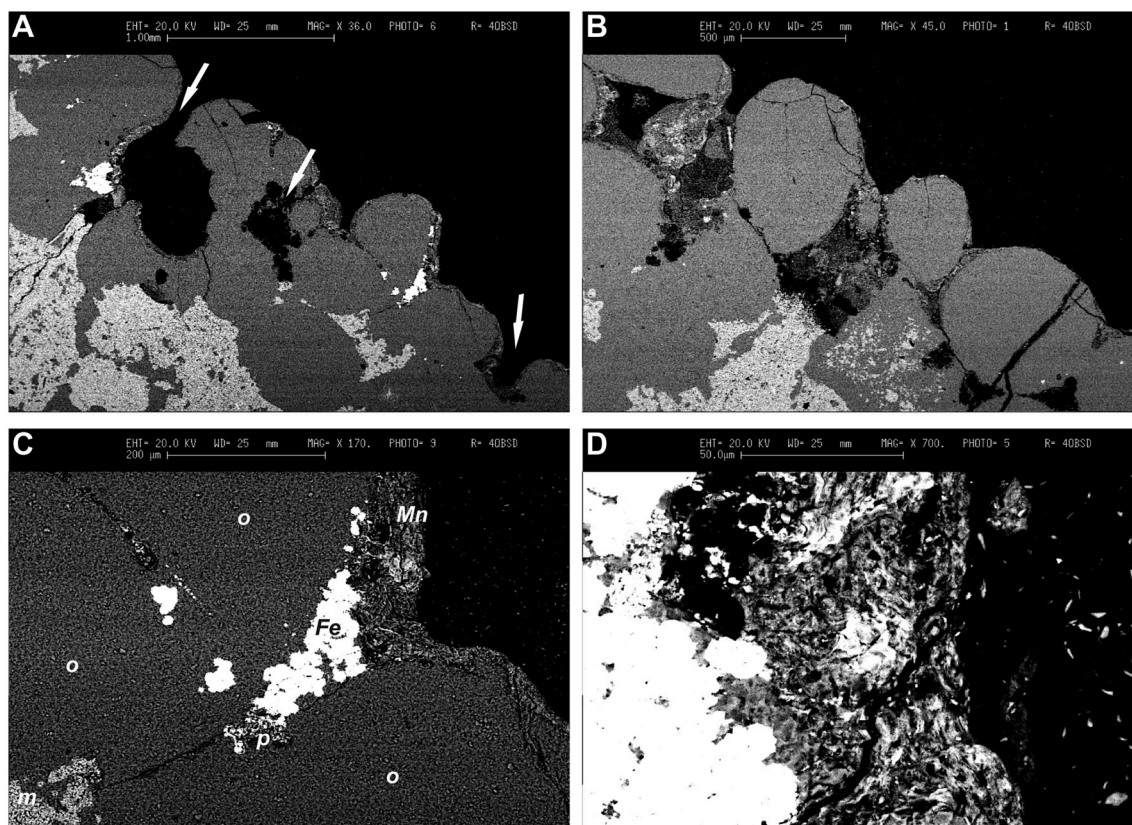


**Fig. 12.** Some examples of Scanning Electron Microscope images of the rock varnish. (A) General view of the varnish infilling dissolution pit and draping grains (indicated by the arrows); notice the presence of silicified ooids and micritic mud. (B) Accumulation of rock varnish inside intergranular spaces. (C) The multi-layered rock varnish described in the text; (o) silicified ooids, (m) micritic muds, (Mn) layer of clay mineral with Mn and Fe oxides, (Fe) Fe-rich layer, (p) accumulation of phosphates. (D) a detail of the transition between the Fe-bearing layer and the Mn-rich one.

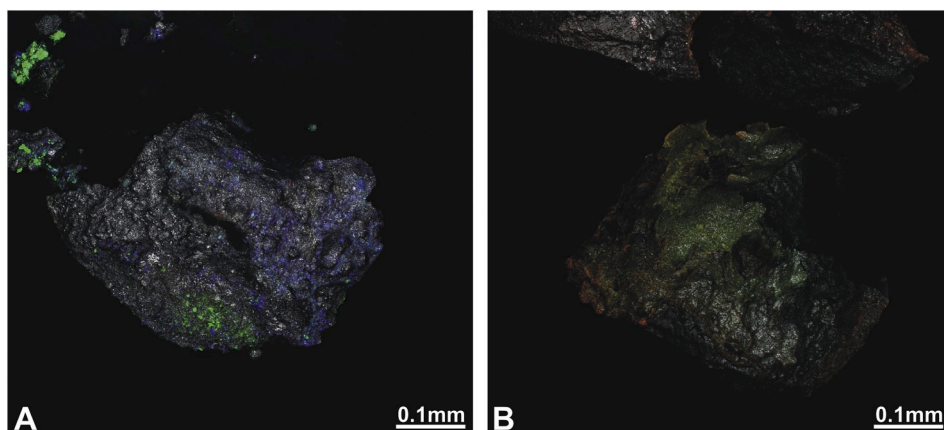


**Fig. 13.** (A) Confocal laser scanning imaging of the biofilm; colours key: phototrophs, red (auto-fluorescence); metabolically active chemotrophs, green (Calcein AM); total chemotrophs, blue (DAPI); stone, grey (reflection). (B) Confocal laser scanning imaging of the extracellular organic matter retrieved on the rock surfaces; colours key: extracellular glycoconjugates, green (Con A); extracellular amine-containing molecules, red (BODIPY® 630/650-X); stone, grey (reflection). (For interpretation of the references to color in this figure legend, the reader is referred to the Web version of this article.)

environmental settings wetter than today, and interrupted by the onset of severe arid climate (Kiersch, 1950; Dorn, 1998, 2007). This is the same environmental context of the Mid-Late Holocene rock varnish formed in the Sahara (Cremaschi, 1996; Zerboni, 2008). Moreover, Krumbrein (1969, 1971) observed rock varnish on silicified limestone from the Negev Desert and, similarly to our case, dissolution created surface pores that were occupied by iron and manganese deposits.

The agent promoting the accumulation of rock varnish could not be unquestionably identified, but we think that a biological mediation occurred. For instance, the surrounded features in the Fe-rich layer are similar to the product of biomineralization (Dorn, 1998). Moreover, a number of studies suggest that a plethora of microbial communities

including bacteria, algae, fungi, and endolithic and epilithic lichens play a role in iron and manganese fixation on both limestone and siliceous bedrocks (Scheffer et al., 1963; Krumbrein, 1969, 1971; Ascaso et al., 1976; Friedmann, 1982; Dorn, 1998). Confocal microscopy images confirmed the presence of a metabolically active microbial community on rock surfaces. These findings also suggest the attribution of rock varnish to biomineralization through the activity of chemotrophs.

### 5.3. Age of rock art and weathering processes, and palaeoenvironmental implications

Once defined the main processes implied in the chemical weathering

of rock surfaces and in the decay of engravings, we can try to delineate a tentative relative chronology of events, which can be improved considering the radiocarbon dating and the comparison with regional palaeoclimatic data.

The single radiocarbon age available refers to the formation of rock varnish. The attribution of the result of radiocarbon dating to rock varnish is suggested by the occurrence of phosphates, whose formation is related to biological processes, trapped within the Fe- and Mn-rich layers. As a consequence, the age of rock varnish formation represents a *terminus ante quem* for the age of engravings. The AMS-<sup>14</sup>C result is also useful in reconstructing the palaeoenvironmental context of rock art.

The oldest process that occurred in the region is the dissolution of limestone, promoted by wet environmental conditions. In the area, most of the Holocene was wetter than today, and arid environmental conditions started in the Late Holocene (e.g. Fleitmann et al., 2007; Cremaschi et al., 2015) also contributing to the abandonment of Early Bronze Age sites and to the transition to a different settlement pattern during the Middle Bronze Age, around c. 2000 BCE (e.g., Magee, 2014). The larger water availability recorded in the Early Bronze Age phase prompted the onset of intensive agriculture and the creation of complex water-management systems (Cremaschi et al., 2018a), and probably allowed the biomineralization of rock varnish in the alveolar voids produced by pristine dissolutions. Likely, the rock surface studied here was engraved during this period. In fact, the available radiocarbon date indicates this happened before 2600 ± 60 uncal. years BP, which means at least before the central part of the local Early Iron Age (overall commonly dated between 1300 and 300 BCE). This is compatible with the identification of a similar representation on an architectural element of the Early Bronze Age tower T2 at Salut, although it only includes isolated halberds and no human figure (Degli Esposti, 2015b).

On the contrary, the subsequent Middle and Late Bronze Age, as well as the Early Iron Age, are marked by a progressive reduction of rainfall (Fleitmann et al., 2007). During this arid period, marked by short-timed wet episodes, biological processes triggering biomineralization were interrupted. Archaeological evidence related to water management and excavation of deep wells confirms the reduction of environmental humidity at the beginning of this long period (Cremaschi et al., 2018a). Likely, short-timed resumption of rainfall occurring in the last three millennia of the Holocene (for instance, in Medieval times) conveyed sufficient water to occasionally reactivate karst dissolution and promote the levelling of the engravings' furrow. Fortunately, the presence of the weathering crust had a case-hardening effect on the underlying rock (*sensu* Kiersch, 1950; Twidale, 1982; Dorn, 1998) preserving engravings up to today. Finally, in the last centuries of severe arid conditions, the wind accreted the thin dust film covering all rock surfaces.

Other means of dating the engravings are admittedly of little help. Comparative dating cannot be used as precise complete parallels are unknown, while the most common isolated halberds also lack a safe date. Stylistic issues seem to be a poor tool, given the overall naïve appearance of the wide majority of the rock art in the region (e.g. Ziolkowski, 2007). Representations of weapons/tools or animals for which dated archaeological counterparts or the age of first domestication are known would be common benchmarks for dating: suffice it to mention the ubiquitous representations of camel-riders and the currently accepted date for the domestication of this animal in ancient Near East around 1000 BCE (Magee, 2015). Unfortunately, there is no evidence in the archaeological record of the area of tools or weapons with a similar shape to the “halberds” depicted in the discussed engravings. The only possible candidate, a tool that actually recalls a small pick-axe, was first known from Mleiha in the Sharjah Emirate (Mouton, 2008), and most recently several examples have been excavated in the Salut plain necropolis (Degli Esposti et al., 2019). The deriving chronology, however, fixed between mid-2nd and 1st century BCE, is strongly incoherent with the radiocarbon determination.

Fossati (2017) has recently proposed a tentative, broad phasing for the rock art of Oman (see also Fig. 2). There, “Dagger in T shape” are

generally linked with 3rd and 2nd millennium BCE engravings. One anchoring point of this hypothesis is the affinity with Yemenite warrior stele, where similar signs actually represent daggers (e.g. Newton and Zarins, 2000). It is clear from the case discussed here, as well as from the Arabah Valley comparison mentioned above, that these T signs cannot be univocally interpreted when found in isolation, and in the present case they surely do not represent daggers. A broad date into the 2nd millennium BCE would, nevertheless, be consistent with the other evidence discussed here.

Fossati's (2017) 6th phase, comprising the long period from the 1st millennium BCE to the present, is distinguished by the widespread representation of warriors (often mounted). If the halberds depicted in the Salut boulder indeed are weapons (nothing precludes different interpretations, such as ceremonial items), their date could thus fit in at the very beginning of this long phase, and possibly suggest an earlier start for it.

## 6. Conclusion

In this paper, we describe a previously unknown iconography in the rock art of the Sultanate of Oman – the man with the halberd –, which does not fit any comparison with the engravings and paintings known in the region, although representations of isolated halberds (also called “Capital T” signs) are, conversely, rather well known (e.g. Ziolkowski, 2007; Fossati, 2017), and are also found scattered over the same oasis of Salut.

We suggest that lithological and environmental reasons are in charge of the scarcity of coeval engravings. The formation of rock varnish is the factor that triggered the preservation of engravings on Jabal Hammah. This process was promoted by the lithology of the boulder – limestone with silicified ooids – as Si-bearing rocks favour the growth of rock varnish. At Jabal Hammah rock varnish was not found on non-silicified limestone surfaces, which are, therefore, more prone to karst dissolution. In such a case, engravings may have been erased. In the area, the few other representations of isolated halberds were found in more protected contexts, as in the case of the engravings on the architectural element of the tower T2. There, the block in the wall was buried after the abandonment of the site and, therefore, the rock surface and engravings did not undergo weathering and dissolution. At Jabal Hammah, the formation of a biomineralized crust preserved engravings from complete erosion triggered by karst dissolution. Many of the blocks and boulders of the area of Salut, however, display strong evidence of this process that might have erased other engravings.

In the case of the studied boulder, the interplay of contrasting chemical and biochemical processes (conservative vs. destructive processes) permitted the preservation of engravings, gave the opportunity to radiocarbon date them, and offered fresh data to reconstruct the complex archaeological landscape of the palaeo-oasis of Salut. Our work also confirms (i) the importance of weathering surfaces as proxy data of past environmental conditions (Dorn, 2007; Cremaschi et al., 2018b), and (ii) the great potential that combined geoarchaeological investigation on rock art and its rock support (Cremaschi, 1996; Cremaschi et al., 2008; Zerboni, 2012) has in palaeoenvironmental reconstruction.

In a broader perspective, our results suggest that in some cases the absence of rock art evidence is not evidence of rock art absence. Destructive natural processes may have acted dismantling or rejuvenating rock surfaces, thus erasing engravings or paintings. Other case studies confirm this general assumption. For instance, in the hyperarid central Sahara, where prehistoric rock art panels and galleries dating to wetter periods of the Holocene are common, some rock shelters settled in prehistoric times do not present any rock art representations, as in the case of the Takarkori Cave (Cremaschi et al., 2014). This is the consequence of climate-driven processes that contributed to the continuous abrasion and dismantling of the friable sandstone surface of the vault of the rock shelter and to the loss of rock art, whose existence is suggested by archaeological evidence discovered in the anthropogenic infilling of

the cave (di Lernia et al., 2016). Future regional rock art studies shall seriously take into account this conclusion.

## Acknowledgments

We would like to express our gratitude to the Office of the Adviser to His Majesty the Sultan for Cultural Affairs, Muscat, and to A. Avanzini, Director of the Italian Mission to Oman (IMTO), whose help made the geoarchaeological research in the region possible. In particular, the Office of the Adviser to His Majesty the Sultan for Cultural Affairs asked M. Cremaschi to perform the rock art survey of the area surrounding the citadel of Salut in year 2016. F. Berra is thanked for helping with the interpretation of the petrography of limestone. Comments from Guest Editors and two reviewers increased the clarity of the manuscript. This research was supported by the Italian Ministry of Education, University, and Research (MIUR) through the project “Dipartimenti di Eccellenza 2018–2022” (WP4 – Risorse del Patrimonio Culturale) awarded to the Dipartimento di Scienze della Terra “A. Desio” of the Università degli Studi di Milano. Financial support for analyses is from Università degli Studi di Milano, Progetto Linea 2 (2017) entrusted to A. Zerboni. The Ministry of Education in Taiwan is kindly acknowledged for funding the PhD of Y.-L. Wu.

## Appendix A. Supplementary data

Supplementary data to this article can be found online at <https://doi.org/10.1016/j.quaint.2019.06.040>.

## References

- Agisoft, 2018. Agisoft Metashape User Manual: Standard Edition. Version 1.5 Copyright © 2018 Agisoft LLC. [https://www.agisoft.com/pdf/metashape\\_1\\_5\\_en.pdf](https://www.agisoft.com/pdf/metashape_1_5_en.pdf).
- Al-Jawhari, N.S., ElMahi, A.T., 2013. Rock engravings at Wadi Al-Jafr, Omna. Significance and meaning (Arabic text). *Adumatu* 27, 29–48.
- Allen, C.D., Groom, K.M., 2013. Evaluation of Grenada's “carib stones” via the rock art stability index. *Appl. Geogr.* 42, 165–175.
- Allen, C.D., Lukinbeal, C., 2011. Practicing physical geography: an actor-network view of physical geography exemplified by the rock art stability index. *Prog. Phys. Geogr.* 35, 227–248.
- Allen, C.D., Cutrell, A.K., Cerveny, N.V., Theurer, J., 2011. Advances in rock art field assessment. *La Pintura* 37, 4–13.
- Alsharhan, A.S., Rizk, Z.A., Niri, A.E.M., Bakhit, D.W., Alhajari, S.A., 2001. Hydrogeology of an Arid Region: the Arabian Gulf and Adjoining Areas. Elsevier, Amsterdam.
- Anati, E., 1968–1974. Rock Art in Central Arabia. Institut Orientaliste, Louvain.
- Ascaso, C., Galvan, J., Ortega, C., 1976. The pedogenic action of *Parmelia conspersa*, *Rhizocarpon geographicum* and *Umbilicaria pustulata*. *Lichenologist* 8, 151–171.
- Ash Shari, A.A., 1994. Dhofar: its Ancient Writings and Inscriptions. Al Ghurair Printing and Publishing House Co, Dubai.
- Avanzini, A., Degli Esposti, M., 2018. Husn Salut and the iron age of south east Arabia. In: Excavations of the Italian Mission to Oman 2004–2014. Arabia Antica 15. L'«Erma» di Bretschneider, Rome, Italy.
- Avanzini, A., Phillips, C., 2010. An outline of recent discoveries at Salut in the Sultanate of Oman. In: Avanzini, A. (Ed.), Eastern Arabia in the first millennium BC, International Conference, Pisa 12th e 13th May 2008. Quaderni di Arabia Antica 3. L'«Erma» di Bretschneider, Rome, Italy, pp. 93–108.
- Avanzini, A., Sedov, A., Condoluci, C., 2005. Salut, sultanate of Oman report (2004–2005). *Egitto e Vicino Oriente* 28, 339–389.
- Bea, M., Angás, J., 2017. Geometric documentation and virtual restoration of the rock art removed in aragón (Spain). *J. Archaeol. Sci.: Report* 11, 159–168. <https://doi.org/10.1016/j.jasrep.2016.11.025>.
- Béchenec, F., 1986. Geological Map of Oman 1:100,000. Sheet NF 40-7A. Bahla. Bureau de recherches géologiques et minières, Orleans, France.
- Bednarik, R.G., 2005. Scientific study of Saudi Arabian rock art. *Rock Art Res* 22, 49–81.
- Bednarik, G.R., 2012. The use of weathering indices in rock art science and archaeology. *Rock Art Science* 29, 59–84.
- Bednarik, R.G., 2017. Scientific investigations into Saudi Arabian rock art: a review. *Mediterr. Archaeol. Archaeometry* 17/4, 43–59.
- Bednarik, R.G., Khan, M., 2002. The Saudi Arabian rock art mission of November 2001. *Atlat* 17, 75–99.
- Cerveny, N., 2005. A Weathering-Based Perspective on Rock Art Conservation. Geography, Arizona State University.
- Clarke, C., 1975a. The rock art of Oman. *J. Oman Stud.* 1, 133–122.
- Clarke, C., 1975b. Rock art in the Oman mountains. *Proc. Sem. Arab. Studies* 5, 13–19.
- Cleuziou, S., Tosi, M., 2000. Ra's al-Jinz and the prehistoric coastal cultures of the Ja'alán. *J. Oman Stud.* 11, 19–73.
- Condoluci, C., Degli Esposti, M., 2015. High places in Oman: the IMTO excavations on Jabal Salut. *Quaderni di Arabia Antica*, vol. 3. L'«Erma» di Bretschneider, Rome, Italy.
- Condoluci, C., Degli Esposti, M., Phillips, C., 2014. Iron age settlement patterns at Salut, ca. 1300–300 BC. *Proc. Sem. Arab. Studies* 44, 99–119.
- Crassard, R., 2013. Prehistoric rock art in hadramawt: the site of ali-1 in wādī bin 'alī (Yemen). *Raydan* 8, 67–72.
- Cremaschi, M., 1996. The rock varnish in the Messak Sattafet (Fezzan, Libyan Sahara), age, archaeological context, and palaeoenvironmental implication. *Geoarchaeology: Int. J.* 11, 393–421.
- Cremaschi, M., Pizzi, C., Zerboni, A., 2008. L'arte rupestre del Tadrart Acacus: testimone e vittima dei cambiamenti climatici. In: di Lernia, S., Zampetti, D. (Eds.), *La Memoria dell'Arte*. Edizioni All'Insegna del Giglio, Firenze, pp. 361–369.
- Cremaschi, M., Zerboni, A., Charpentier, V., Crassard, R., Isola, I., Regattieri, E., Zanchetta, G., 2015. Early Holocene climate changes and pre-Neolithic human occupations as recorded in the cavities of Jebel Qara (Dhofar, southern Sultanate of Oman). *Quaternary International* 382, 264–276.
- Cremaschi, M., Zerboni, A., Mercuri, A.M., Olmi, L., Biagetti, S., di Lernia, S., 2014. Takarkori rock shelter (SW Libya): an archive of Holocene climate and environmental changes in the central Sahara. *Quat. Sci. Rev.* 101, 36–60.
- Cremaschi, M., Degli Esposti, M., Fleitmann, D., Perego, A., Sibilia, E., Zerboni, A., 2018a. Late Holocene onset of intensive cultivation and introduction of the falaj irrigation system in the Salut oasis (Sultanate of Oman). *Quat. Sci. Rev.* 200, 123–140. <https://doi.org/10.1016/j.quascirev.2018.09.029>.
- Cremaschi, M., Trombino, L., Zerboni, A., 2018b. Palaeosoils and relict soils, a systematic review. In: Stoops, G., Marcelino, V., Mees, F. (Eds.), *Interpretation of Micromorphological Features of Soils and Regoliths – Revised Edition*. Elsevier, Amsterdam, pp. 863–894. <https://doi.org/10.1016/B978-0-444-63522-8.00029-2>.
- Darvill, T., Batarda Fernandes, A.P., 2014. Open-air Rock-Art Conservation and Management. State of the Art and Future Perspectives. Routledge, London.
- De Cardi, B., Collier, St. Doe, B., 1976. Excavations and survey in Oman, 1974–1975. *J. Oman Stud.* 2, 101–188.
- de Ceuninck, G., 1998. Les pétroglyphes du Fujairah, emirates arabes unis. In: Phillips, C. S., Potts, D.T., Searight, S. (Eds.), *Arabia and its neighbours. Essays on prehistorical and historical developments presented in honour of Beatrice de Cardi*, vol. 2. Abiel, Leiden, Brepols, pp. 33–45.
- De Reu, J., Plets, G., Verhoeven, G., De Smedt, P., Bats, M., Cherretté, B., De Maeyer, W., Deconynck, J., Herremans, D., Laloo, P., Van Meirvenne, M., De Clercq, W., 2013. Towards a three-dimensional cost-effective registration of the archaeological heritage. *J. Archaeol. Sci.* 40, 1108–1121. <https://doi.org/10.1016/j.jas.2012.08.040>.
- Degen, T., Sadki, M., Bron, E., König, U., Nénert, G., 2014. The highscore suite. *Powder Diff.* 29, S13–S18.
- Degli Esposti, M., 2012. The excavation of an early Bronze age tower near Salut (bisayah, sultanate of Oman): the iron age levels. *Egitto e Vicino Oriente* 34, 189–224.
- Degli Esposti, M., 2015a. Two thousand years of settlement at Salut (ca. 2300–300 BC). In: Avanzini, A. (Ed.), *In the Heart of Oman. The Castle of Salut*. (Ancient Oman, 1). L'«Erma» di Bretschneider, Roma, Italy, pp. 55–66.
- Degli Esposti, M., 2015b. Iron age seals from ST1 and Salut, central Oman. *Egitto e Vicino Oriente* 37, 133–147.
- Degli Esposti, M., 2016. Excavations at the Early Bronze Age site «ST1» near Bisayah (Sultanate of Oman): notes on the architecture and material culture. In: Stucky, R.A., Kaelin, O., Mathys, H.-P. (Eds.), *Proceedings of the 9th International Congress on the Archaeology of the Ancient Near East*. June 9–13, 2014. University of Basel, vol. 3. Harrassowitz Verlag, Wiesbaden, Germany, pp. 665–678.
- Degli Esposti, M., Ramorino, P., Spano, S., Tagliamonte, E., (in press). Funerary archaeology at Salut (Oman) 2017–2018. Insights on Middle Bronze Age grave's architecture and a possible new type of third millennium grave. *Egitto e Vicino Oriente* 41.
- Degli Esposti, M., Condoluci, C., Phillips, C., Tagliamonte, E., Sasso, M., 2018a. The early Iron age chronology in south east Arabia: a reassessment on the basis of Husn Salut excavations. In: Avanzini, A., Degli Esposti, M. (Eds.), *Husn Salut and the Iron Age of South East Arabia*. Excavations of the Italian Mission to Oman 2004–2014. Arabia Antica 15. L'Erma di Bretschneider, Roma, pp. 371–382.
- Degli Esposti, M., Cremaschi, M., Perego, A., Zerboni, A., 2018b. Geographical and environmental setting. In: Avanzini, A., Degli Esposti, M. (Eds.), *Husn Salut and the Iron Age of South East Arabia*. Excavations of the Italian Mission to Oman 2004–2014. Arabia Antica 15. L'Erma di Bretschneider, pp. 19–31.
- Degli Esposti, M., Tagliamonte, E., Sasso, M., Ramorino, P., 2019. The late iron age of central Oman (c. 300BC–300AD) — new insights from salut. *Proc. Seminar Arab. Stud.* 49, 97–113.
- di Lernia, S., Bruni, S., Cislighi, I., Cremaschi, M., Gallinaro, M., Guglielmi, V., Mercuri, A.M., Poggi, G., Zerboni, A., 2016. Colour in context. Pigments and other coloured residues from the Early-Middle Holocene site of Takarkori (SW Libya). *Archaeol. Anthropol. Sci.* 8, 381–402.
- Dorn, R.I., 1998. Rock Coatings. *Developments in Earth Surface Processes* 6. Elsevier, Amsterdam.
- Dorn, R.I., 2006. Petroglyphs in Petrified Forest National Park: role of rock coatings as agents of sustainability and as indicators of antiquity. *Bull. Mus. North Ariz.* 63, 53–64.
- Dorn, R.I., 2007. Rock varnish. In: Nash, J.D., McLaren, S.J. (Eds.), *Geochemical Sediments & Landscape*. Blackwell Publishing, Oxford, UK, pp. 246–297.
- Dorn, R.I., Jull, A.J.T., Donahue, D.J., Linick, T.W., Toolin, L.J., 1989. Accelerator mass spectrometry radiocarbon dating of rock varnish. *Geol. Soc. Am. Bull.* 101, 1363–1372.

- Dorn, R.I., Clarkson, P.B., Nobbs, M.F., Loendorf, L.L., Whitley, D.S., 1992. New approach to the radiocarbon dating of rock varnish, with examples from drylands. *Ann. Assoc. Am. Geogr.* 82, 136–151.
- Dorn, R.I., Whitley, D.S., Cerveny, N.V., Gordon, S., Casey, D.A., Gutbrod, E., 2008. The rock art stability index. *Herit. Manag.* 1, 35–70.
- Engel, C.G., Sharp, R.S., 1958. Chemical data on desert varnish. *Geol. Soc. Am. Bull.* 69, 487–518.
- Fiol, L., Fornos, J., Ginés, A., 1992. El Rilkenkarren: un tipus particular de biocars? Primaries dades. *Endins* 17–18, 43–49.
- Fleitmann, D., Burns, S.J., Mangini, A., Mudelsee, M., Kramers, J., Villa, I., Neff, U., Al-Subbarye, A.A., Buettner, A., Hippler, D., Matter, A., 2007. Holocene ITCZ and Indian monsoon dynamics recorded in stalagmites from Oman and Yemen (Socotra). *Quat. Sci. Rev.* 26, 170–188.
- Fossati, A.E., 2017. Current finds in rock art research of Oman: a review and update. *Mediterr. Archaeol. Archaeometry* 17/4, 75–88.
- Friedmann, E.I., 1982. Endolithic microorganisms in the Antarctic cold desert. *Science* 215, 1045–1053.
- Galeazzi, F., 2016. Towards the definition of best 3D practices in archaeology: assessing 3D documentation techniques for intra-site data recording. *J. Cult. Herit.* 17, 159–169.
- Gallinaro, M., Zerbini, A., Solomon, T., Spinapolice, E.E., 2018. Rock art between preservation, research and sustainable development – a perspective from Southern Ethiopia. *Afr. Archaeol. Rev.* 35, 211–223. <https://doi.org/10.1007/s10437-018-9289-z>.
- Giesen, M.J., Ung, A., Warke, P.A., Christgen, B., Mazel, A.D., Graham, D.W., 2014. Condition assessment and preservation of open-air rock art panels during environmental change. *J. Cult. Herit.* 15, 49–56.
- Ginés, A., Knez, M., Slabe, T., Dreybrodt, W., 2009. Karst Rock Features: Karren Sculpturing. Založba ZRC, Ljubljana.
- Glennie, K.W., Boeuf, M.G.A., Hughes Clarke, M.W., Moody-Stuart, M., Pilaar, W.F.H., Reinhardt, B.M., 1974. Geology of the Oman Mountains, vol. 31. Koninklijk Nederlands Geologisch Mijnbouwkundig Genootschap, Amsterdam.
- Groom, K.M., 2016. The applicability of repeat photography in rock art conservation: a case study of mixed methods in the Arkansas Ozarks. *Z. Geomorphol.* 60 (Suppl. 3), 011–028.
- Groom, K.M., 2017. Rock Art Management and Landscape Change: Mixed Field Assessment Techniques for Cultural Stone Decay. PhD dissertation. University of Arkansas.
- Groom, K.M., Thompson, T.J., 2011. RASI Survey of Sites in Petrified Forest National Park 2011. National Park Service, Rocky Mountain Cooperative Ecosystem, Study Unit Project Summary Report.
- Guagnin, M., Shipton, C., al-Rashid, M., Moussa, F., El-Dossary, S., Sleight, M.B., Alsharekh, A., Petraglia, M., 2017. An illustrated prehistory of the Jubbah oasis: reconstructing Holocene occupation patterns in north-western Saudi Arabia from rock art and inscriptions. *Arabian Archaeol. Epigr.* 28, 138–152.
- Haerick, E., 1998. Petroglyphs at sanidil in the hajjar mountains (southeast Arabia). In: Phillips, C.S., Potts, D.T., Searight, S. (Eds.), *Arabia and its neighbours. Essays on prehistorical and historical developments presented in honour of Beatrice de Cardi*. (Abiel 2). Leiden, Brepols, pp. 79–87.
- Hall, K., Meiklejohn, I., Arocena, J., Prinsloo, L., Sumner, P., Hall, L., 2007. Deterioration of San rock art: new findings, new challenges. *South Afr. J. Sci.* 103, 9–10.
- Hall, K., Meiklejohn, I., Sumner, P., Arocena, J., 2009. Light penetration into Clarens sandstone and implications for deterioration of San rock art. *Geoarcheology: Int. J.* 25, 122–136.
- Hastings, A., Humphries, J.H., Meadow, R.H., 1975. Oman in the third millennium BCE. *J. Oman Stud.* 1, 9–55.
- Hein, J.R., Koski, R.A., 1987. Bacterially mediated diagenetic origin for chert-hosted manganese deposits in the Franciscan Complex, California Coast Ranges. *Geology* 15, 722–726.
- Hooke, R.L., Yang, H., Weiblen, P.W., 1969. Desert varnish: an electron probe study. *J. Geol.* 77, 275–288.
- Howard, A.J., 2013. Managing global heritage in the face of future climate change: the importance of understanding geological and geomorphological processes and hazards. *Int. J. Herit. Stud.* 19, 632–658.
- Insall, D., 1999. The petroglyphs of Shenah. *Arabian Archaeol. Epigr.* 10, 225–245.
- Jalandoni, A., Domingo, I., Taçon, P.S.C., 2018. Testing the value of low-cost Structure-from-Motion (SfM) photogrammetry for metric and visual analysis of rock art. *J. Archaeol. Sci.: Report* 17, 605–616. <https://doi.org/10.1016/j.jasrep.2017.12.020>.
- Jäckli, R., 1980. Rock Art in Oman. An Introductory Presentation. Manuscript submitted to the Ministry of Heritage and Culture, Muscat, Oman.
- Jennings, R.C., Shipton, C., Al-Omari, A., Alsharekh, A.M., Crassard, M., Groucutt, H., Petraglia, M.D., 2013. Rock art landscapes beside the Jubbah palaeolake, Saudi Arabia. *Antiquity* 87, 666–683.
- Johnson, R.A., Solis, A., 2016. Using photogrammetry to interpret human action on Neolithic monument boulders in Ireland's Cavan Burren. *J. Archaeol. Sci.: Report* 8, 90–101. <https://doi.org/10.1016/j.jasrep.2016.05.055>.
- Jung, M., 1994. On representations of camels and camel-riders in the rock art of Northern Yemen. *East W.* 44 (2–4), 231–248.
- Khan, M., 2007. The Rock Art of Saudi Arabia across Twelve Thousand Years. Ministry of Education, Kingdom of Saudi Arabia.
- Khan, M., 2013. Rock art of Saudi Arabia. *Arts* 2, 447–475.
- Kiersch, G.A., 1950. Small-scale structures and other features of the Navajo Sandstone, northern part of the San Rafael Swell, Utah. *Bull. Am. Assoc. Petrol. Geol.* 34, 923–942.
- Kranjc, A., 2010. Arid karst or karst in arid countries? *Egypt. J. Environ. Chang.* 2, 43–46.
- Krumbein, W.E., 1969. Ober den Einfluss der Mikroflora auf die Exogene Dynamik (Verwitterung und Krustenbildung). *Geol. Rundsch.* 58, 333–363.
- Krumbein, W.E., 1971. Biologische Entstehung von wiistenlack. *Umschau* 71, 210–211.
- Macholdt, D.S., Jochum, K.P., Al-Amri, A., Andraea, M.O., (in press). Rock varnish on petroglyphs from the Hima region, southwestern Saudi Arabia: chemical composition, growth rates, and tentative ages. *Holocene*.
- Magee, P., 2014. *The Archaeology of Prehistoric Arabia. Adaptation and Social Formation from the Neolithic to the Iron Age*. Cambridge University Press, Cambridge.
- Magee, P., 2015. When was the dromedary domesticated in the ancient Near East? *Z. für Orient-Archäol.* 8, 253–278.
- Mol, L., Preston, P.R., 2010. The writing's in the wall: a review of new preliminary applications of electrical resistivity tomography within archaeology. *Archaeometry* 52, 1079–1095.
- Mouton, M., 2008. La péninsule d'Oman de la fin de l'Âge du fer au début de la période Sassanide (250 av.–350 ap. JC). *British Archaeological Reports, International Series* 1776. Archaeopress, Oxford.
- Munsell®, 1994. *Soil Color Charts. 1994 Revised Edition*. Munsell® Color, New Windsor, ST, USA.
- Murphy, C.P., 1986. *Thin Section Preparation of Soils and Sediments*. AB Academic Publishers, Berkhamsted, Herts.
- Nayeem, M.A., 2000. *The Rock Art of Arabia: Saudi Arabia, Oman, Qatar, the Emirates & Yemen*. Hyderabad Publishers, Hyderabad, India.
- Neff, U., Burns, S.J., Mangini, A., Mudelsee, M., Fleitmann, D., Matter, A., 2001. Strong coherence between solar variability and the monsoon in Oman between 9 and 6 ka ago. *Nature* 411, 290–293.
- Newton, L.S., Zarins, J., 2000. Aspects of Bronze Age art of southern Arabia: the pictorial landscape and its relation to economic and socio-political status. *Arabian Archaeol. Epigr.* 11, 154–179.
- Nriagu, J.P., 1984. Phosphate minerals: their properties and general modes of occurrence. In: Nriagu, J.P., Moore, P.B. (Eds.), *Phosphate Minerals*. Springer-Verlag, Berlin, pp. 1–136.
- Orchard, J.J., Orchard, J.C., 2002. The work of the Al-Hajar project in Oman. *J. Oman Studies* 12, 227–234.
- Orchard, J.C., Stanger, G., 1994. Third millennium oasis towns and environmental constraints on settlement in the Al-Hajar region. *Iraq* 56, 63–100.
- Peña-Villaseñin, S., Gil-Docampo, M., Ortiz-Sanz, J., (in press). Professional SfM and TLS vs a simple SfM photogrammetry for 3D modelling of rock art and radiance scaling shading in engraving detection. *J. Cult. Herit.* <https://doi.org/10.1016/j.culher.2018.10.009>.
- Phillips, C., Condoluci, C., Degli Esposti, M., 2010. Archaeological survey in wadi Bahla (sultanate of Oman): an iron age site on jabal al-agma, near bisyah. *Egitto e Vicino Oriente* 33, 151–168.
- Phillips, C., Condoluci, C., Degli Esposti, M., 2012. Further consideration of Bronze and iron age settlement patterns at Salut. *Egitto e Vicino Oriente* 35, 193–217.
- Phillips, C., Condoluci, C., Degli Esposti, M., 2015. Works of the Italian Mission at Salut: a concise overview of ten years of investigation. In: Avanzini, A. (Ed.), *In the Heart of Oman. The Castle of Salut. Ancient Oman 1. L'Erma* di Bretschneider, Rome, Italy, pp. 35–54.
- Plisson, H., Zotkina, L.V., 2015. From 2D to 3D at macro- and microscopic scale in rock art studies. *Digital applications in archaeology and cultural heritage*. <https://doi.org/10.1016/j.daach.2015.06.002>.
- Potter, R.M., Rossman, G.R., 1979. The manganese- and iron-oxide mineralogy of desert varnish. *Chem. Geol.* 25, 79–24.
- Preston, K., 1976. An introduction to the anthropomorphic content of the rock art of Jebel Akhdar. *J. Oman Stud.* 2, 17–38.
- Reimer, P.J., Bard, E., Bayliss, A., Beck, J.W., Blackwell, P.G., Bronk Ramsey, C., Buck, C.E., Cheng, H., Edwards, R.L., Friedrich, M., Grootes, P.M., Guilderson, T.P., Hafflidason, H., Hajdas, I., Hatt e, C., Heaton, T.J., Hoffmann, D.L., Hogg, A.G., Hughen, K.A., Kaiser, K.F., Kromer, B., Manning, S.W., Niu, M., Reimer, R.W., Richards, D.A., Scott, E.M., Southon, J.R., Staff, R.A., Turney, C.S.M., Plicht, J., 2013. IntCal13 and Marine13 radiocarbon age calibration curves 0–50,000 years cal BP. *Radiocarbon* 55, 1869–1887.
- Reneau, S.L., Raymond, R., Harrington, C.D., 1992. Elemental relationships in rock varnish stratigraphic layers, Cima Volcanic Field, California, implications for varnish development and the interpretation of varnish chemistry. *Am. J. Sci.* 292, 684–723.
- Rigaku Oxford Diffraction, 2018. *CrysAlisPro Software System, Version 1.171.33.41*. Rigaku Corporation, Oxford, UK.
- Rivard, B., Arvidson, R.E., Duncan, I.J., Sultan, M., Kaliouby, B., 1992. Varnish, sediment, and rock controls on spectral reflectance of outcrops in arid regions. *Geology* 20, 295–298.
- Robert, E., Petrogiani, S., Lesvignes, E., 2016. Applications of digital photography in the study of Paleolithic Cave art. *J. Archaeol. Sci.: Report* 10, 847–858. <https://doi.org/10.1016/j.jasrep.2016.07.026>.
- Rothenberg, B., 1972. *Timna. Valley of the Biblical Copper Mines. New Aspects of Antiquity*. Thames & Hudson, London.
- Rothenberg, B., 2001. Rock drawings in the Ancient Copper Mines of the Arabah - new aspects of the region's history. *IAMS* 21, 4–9.
- Rothenberg, B., Tylecote, R.F., Boydell, P.J., 1978. *Chalcolithic Copper Smelting. IAMS Monographs 1*. IAMS, London.
- Sanz, J.O., de la Luz Gil Docampo, M., Martínez Rodríguez, S., Rego Sanmartín, M.T., Mejiide Cameselle, G., 2010. A simple methodology for recording petroglyphs using low-cost digital image correlation photogrammetry and consumer-grade digital

- cameras. *J. Archaeol. Sci.* 37, 3158–3169. <https://doi.org/10.1016/J.JAS.2010.07.017>.
- Scheffer, F., Meyer, B., Kalk, E., 1963. Biologische ursachen der wiistenlackbildung. *Z. Geomorphol.* 7, 112–119.
- Smith, B.J., 1988. Weathering of superficial limestone debris in a hot desert environment. *Geomorphology* 1, 355–367.
- Sowers, J.M., 2000. Rock varnish chronometry. In: Noller, J.S., Sowers, J.M., Lettis, W.R. (Eds.), *Quaternary Geochronology: Methods and Applications*. American Geophysical Union Reference Shelf 4, Washington, pp. 241–260.
- Tagliamonte, E., Avanzini, A., 2018. New data from the renewed excavation at salūt: the iron age settlement (Qaryat salūt). *Proc. Sem. Arab. Studies* 48, 339–351.
- Tokunaga, R., Fujii, S., Adachi, T., 2019. Early islamic and ancient north arabian graffiti and petroglyphs in tabūk province - Saudi-Japanese al-jawf/tabūk archaeological project (JTAP), march 2017 field season. *Proc. Seminar Arab. Stud.* 49, 275–282.
- Twidale, C.R., 1982. *Granite Landforms*. Elsevier, Amsterdam.
- Waagen, J., 2019. New technology and archaeological practice. Improving the primary archaeological recording process in excavation by means of UAS photogrammetry. *J. Archaeol. Sci.* 101, 11–20. <https://doi.org/10.1016/j.jas.2018.10.011>.
- Walkley, A., Black, I.A., 1934. An examination of Degtjareff method for determining soil organic matter and a proposed modification of the chromic acid titration method. *Soil Sci.* 37, 29–38.
- Weyhenmeyer, C.E., Burns, S.J., Waber, H.N., Aeschbach-Hertig, W., Kipfer, R., Loosli, H., Matter, A., 2000. Cool glacial temperatures and changes in moisture source recorded in Oman groundwaters. *Science* 287, 842–845.
- Weyhenmeyer, C.E., Burns, S.J., Waber, H.N., Macumber, P.G., Matter, A., 2002. Isotope study of moisture sources, recharge areas, and groundwater flow paths within the eastern Batinah coastal plain, Sultanate of Oman. *Water Resour. Res.* 38, 1184.
- Whitcomb, D.S., 1975. The archaeology of Oman: a preliminary discussion of the Islamic periods. *J. Oman Studies* 1, 123–158.
- Whitley, S.D., 2005. *Introduction to Rock Art Research*. Left Coast Press, Walnut Creek, CA, USA.
- Yule, P.A., 2001. The hasat bin salt in the al-zahirah province of the sultanate of Oman. In: Boehmer, R.M., Maran, J. (Eds.), *Lux Orientis. Archäologie zwischen Asien und Europa. Festschrift für Harald Hauptmann zum 65 Geburtstag*. Internationale Archäologie 12. Verlag Marie Leidorf, Rahden/Westf., pp. 443–450.
- Zerboni, A., 2008. Holocene rock varnish on the Messak plateau (Libyan Sahara): chronology of weathering processes. *Geomorphology* 102, 640–651. <https://doi.org/10.1016/j.geomorph.2008.06.010>.
- Zerboni, A., 2012. Rock art from the central Sahara (Libya): a geoarchaeological and palaeoenvironmental perspective. In: Huyge, D., Van Noten, F., Swinne, D. (Eds.), *Proceedings of the International Colloquium ‘The Signs of Which Times? Chronological and Palaeoenvironmental Issues in the Rock Art of Northern Africa* (Brussels, 3-5 June 2010). Royal Academy for Overseas Sciences, Brussels, pp. 175–195.
- Ziolkowsky, M., 1998. A study of the petroglyphs from Wadi al-Hayl, Fujairah, United Arab Emirates. *Arabian Archaeol. Epigr.* 9, 13–89.
- Ziolkowsky, M., 2007. Rock on art: petroglyph sites in the United Arab Emirates. *Arabian Archaeol. Epigr.* 18, 208–238.